Conductivity of molten sodium chloride in an alternating electric field

Janka Petravic and Jérôme Delhommelle

Citation: The Journal of Chemical Physics **119**, 8511 (2003); doi: 10.1063/1.1613256
View online: http://dx.doi.org/10.1063/1.1613256
View Table of Contents: http://scitation.aip.org/content/aip/journal/jcp/119/16?ver=pdfcov
Published by the AIP Publishing

Conductivity of molten sodium chloride in an alternating electric field

Janka Petravic[a)]
Research School of Chemistry, The Australian National University, Building 35, Science Road, Canberra ACT 0200, Australia

Jérôme Delhommelle
Équipe de Chimie et Biochimie Théoriques, UMR 7565, Université Henri Poincaré, BP 239, F-54506 Vandœuvre-lès-Nancy Cedex, France

(Received 3 July 2003; accepted 1 August 2003)

We study the properties of molten sodium chloride in alternating electric fields of two amplitudes and for a large range of frequencies using nonequilibrium molecular dynamics simulations, and compare the responses with two different methods of temperature control to the predictions of linear response theory. We find that the considerable nonlinearity in the resulting current density observed at low frequencies can be explained by the characteristics of the nonlinear response to constant fields. We also comment on the differences in the dissipation mechanisms and the entropy change with two thermostats. © *2003 American Institute of Physics.* [DOI: 10.1063/1.1613256]

I. INTRODUCTION

This paper is a result of our continuing interest in the properties of the response of ionic liquids to strong external perturbations.[1,2] In this work our aim is to study the time-dependent response of a representative ionic liquid to an alternating electric field, depending on the field amplitude and frequency. The fields employed in nonequilibrium molecular dynamics (NEMD) simulations are huge when translated into macroscopic conditions, and often inaccessible to experiments. Our previous results indicate that the way heat dissipation is simulated becomes important in strong external fields, when the energy dissipation during the characteristic relaxation time becomes comparable to the internal energy itself, and when allowing for the flow fluctuations contributes to formation of the response. Therefore, in addition to the electric current, we investigate in more detail how the process of heat exchange with environment is represented by different types of thermostats.

The frequency and wave vector dependence of equilibrium density and charge fluctuations in ionic liquids has attracted interest from the early days of molecular dynamics simulations, from the studies on idealized systems[3] to the recent realistic studies of their dependence on mass and size differences and their relationship to frequency-dependent electrical conductivity.[4]

The only NEMD simulation of an ionic liquid in an alternating electric field that we are aware of was performed on an idealized model monovalent ionic liquid with ions of equal mass and size[5] in a relatively low amplitude and high frequency field, with a Gauss type of thermostat applied relative to the mean flow velocity of each type of ion. For this system, frequency-dependent conductivity was found to agree with the Fourier decomposition of the equilibrium current autocorrelation function and exhibit a maximum at a characteristic frequency value.

a)Electronic mail: janka@rsc.anu.edu.au

II. DEFINITIONS OF TEMPERATURE AND EQUATIONS OF MOTION

In an NEMD simulation, a system is typically subjected to an external perturbation and the response is measured directly. In order to remove the Joule heating in NEMD simulations of bulk systems, a thermostat term is added to the equations of motion. This term provides feedback control of a microscopic expression for temperature. The temperature that is usually controlled is the ''kinetic temperature,'' defined in terms of velocity fluctuations relative to flow velocity. In an electric field, kinetic temperature T_{KIN} is expressed in terms of momenta relative to the flow velocity of each type of ion[6]

$$\frac{3}{2}Nk_{\mathrm{B}}T_{\mathrm{KIN}}=\sum_{\nu=+,-}\frac{1}{2m_{\nu}}\left\langle\sum_{i\nu=1}^{N}(\mathbf{p}_{i\nu}-m_{\nu}\mathbf{u}_{\nu})^{2}\right\rangle, \tag{1}$$

where $\mathbf{u}_{\nu}$ is the flow velocity of each type, N is the total number of ions, k_{B} is the Boltzmann constant, $\nu=+,-$ denotes cations and anions, m_{ν} is the mass of the ion of type ν, $\mathbf{p}_{i\nu}$ is the momentum of ion i, and the index $i\nu$ goes over ions of type ν only. The angular brackets $\langle ...\rangle$ denote the ensemble average. It is assumed that there are $N/2$ ions of each type. Note that the flow velocity $\mathbf{u}_{\nu}$ in the definition of T_{KIN} is the instantaneous value of the average velocity of ions of type ν. It is implicitly assumed that the flow velocity is the same throughout the simulation box and depends only on time.

In order to make the desired kinetic temperature an exact constant of motion, we used the Gauss minimal constraint method.[7,8] The electric field is applied in the x direction. The equations of motion in this case are of the form

$$\begin{aligned}\dot{\mathbf{r}}_i&=\mathbf{p}_i/m_i,\\ \dot{\mathbf{p}}_i&=\mathbf{F}_i+\mathbf{i}z_i eE_{\mathrm{EL}}(t)-\alpha\mathbf{p}_i,\end{aligned} \tag{2}$$

where $\mathbf{r}_i$, $\mathbf{p}_i$, and m_i are position, momentum, and mass of ion i, respectively, z_i is its formal charge, and e is the elec-

tron charge, $\mathbf{F}_i$ is the total force on ion i resulting from the interaction potential, $E_{\mathrm{EL}}(t)$ is the time-dependent magnitude of electric field, $\mathbf{i}$ is the unit vector in the x direction, and α is the thermostat multiplier. The expressions for the thermostat multiplier α are given in Refs. 2 and 9.

In weak fields flow velocity is relatively easy to determine, but in strong fields, when it becomes space- and time-dependent, it is not a simple matter to decide which part of particle velocity is due to the flow and which is thermal motion. This problem is generally considered to be more important in strongly sheared systems,[10] where the assumed linear velocity profile changes with increase of the shear rate. However, in the electrical conductivity simulations, the thermostat directly affects the response, i.e., the electric current, and our results for the field-dependent electrical conductivity in molten salts[2] indicate that flow fluctuations are important in establishing the steady-state current in a constant electric field.

An alternative configurational representation expresses temperature[11,12] only in terms of positions, which avoids the problem of finding the flow velocity. In equilibrium, both expressions are equivalent and can be derived from thermodynamic definition. If we assume that far from equilibrium local equilibrium still holds, we can use the equilibrium expressions for temperature even in strong flows. When configurational temperature is maintained constant, the value of kinetic expression increases because it contains the fluctuating flow velocities as well as thermal velocities. The difference is an indication of the importance of spatial and temporal flow fluctuations. On the other hand, when kinetic temperature is kept constant, configurational temperature can differ either way,[1,2] depending on how suppressing flow fluctuations affects the fluid structure.

The approximate definition of configurational temperature T_{CONF}

$$k_{\mathrm{B}}T_{\mathrm{CONF}}=-\left\langle \sum_{i=1}^{N}\mathbf{F}_i^2\right\rangle \Big/ \left\langle \sum_{i=1}^{N}\nabla_i\cdot\mathbf{F}_i\right\rangle, \tag{3}$$

should in equilibrium agree with the kinetic definition (1) up to terms of order $1/N$. In our case the agreement was better than 0.1%.

The ''configurational'' thermostat is introduced using the Nosé–Hoover integral type of feedback.[12,13] The thermostat multiplier is in the position equations of motion because configurational temperature is defined in terms of positions

$$\dot{\mathbf{r}}_i=\frac{\mathbf{p}_i}{m_i}+\frac{\xi}{T_0}\frac{\partial T_{\mathrm{CONF}}}{\partial \mathbf{r}_i}, \tag{4a}$$

$$\dot{\mathbf{p}}_i=\mathbf{F}_i+\mathbf{i}z_i eE_{\mathrm{EL}}, \tag{4b}$$

$$\dot{\xi}=-\frac{\sigma^2}{\tau_{TC}^2}\frac{(T_{\mathrm{C1}}-T_0)}{T_0}. \tag{4c}$$

In (4c), σ is the mean particle exclusion diameter and τ_{TC} is the response time of the feedback mechanism. Since $\nabla^2(1/r)=0$, electrostatic interactions do not contribute directly either to the thermostat terms in (4a) or to the numerator of (3).

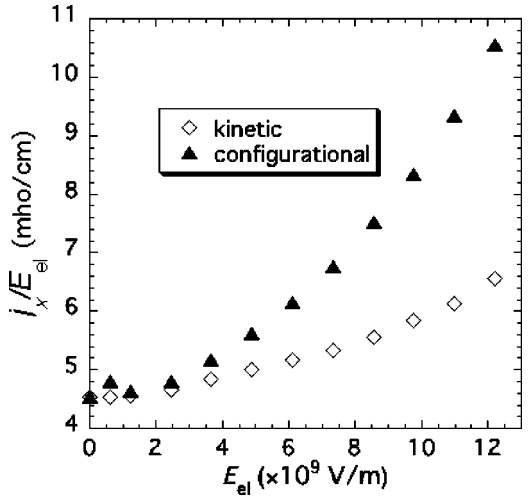

FIG. 1. Dependence of dc conductivity of molten NaCl on electric field with kinetic and configurational thermostat.

III. THE MODEL AND TECHNICAL DETAILS

Our model ionic system represents molten sodium chloride described by the Born–Huggins–Mayer potential with the parameters determined by Fumi and Tosi.[14] We studied its properties at temperature of 1500 K and density of 1.5 g/cm^3, a state point close to the middle of the liquid region of the phase diagram,[15] for two electric field amplitudes, 4.88×10^9 V/m and 12.2×10^9 V/m. The field-dependent conductivity in constant electric fields, including these two fields, for the same system has already been computed in our previous study[2] and is used here for comparison with the low frequency results. Both fields are in the nonlinear response region in the zero-frequency limit, but for the lower one there is a near agreement of currents with different thermostats, while with the higher field there are large quantitative differences. The nonlinearity of the field dependence of the current is much stronger for configurational thermostat, suggesting that local fluctuations of current are important for conductivity[2] (Fig. 1).

Molecular dynamics simulations were performed on systems consisting of 512 ions (256 ions of each type). The system of first-order equations of motion was solved using the fifth-order Gear predictor–corrector scheme. Electrostatic interactions were treated using the Ewald summation technique with the conducting boundary at infinity.[16] The nonelectrostatic and the real-space electrostatic interactions were cut off at half the box length, $L/2$, the reciprocal space wave vector cutoff was at $k_{\max}=6(2\pi/L)$, and the convergence acceleration factor was chosen as $\kappa=1.8\pi/L$. Beyond the cutoff, the long-range corrections to the nonelectrostatic contribution to potential energy and hydrostatic pressure were included in order to account for the truncation effects.[17] The system was started off as an fcc lattice at the correct density and first equilibrated for 0.5 ns.

For simulations in the alternating field, the integration time step was either one-hundredth of the period of the field, or 1 fs, whichever was smaller, except for the higher field of the three lowest frequencies with configurational thermostat, where it had to be reduced to 0.1 fs because of numerical instabilities. The value of the feedback constant in configurational thermostat σ^2/τ_{TC}^2 was 100 $\text{Å}^2/\text{ps}^2$, except for the higher field of the three lowest frequencies where it needed to be increased to 1000 $\text{Å}^2/\text{ps}^2$. The final periodic state was judged to be reached after 100 periods of the field, when the averages over a period were collected. The averaging was done over at least 1000 periods for frequencies higher than 1 ps^{-1}, and at least 125 periods for the lowest frequencies.

IV. LINEAR RESPONSE

In a steady state in an external electric field E_{EL} applied along the x axis, oppositely charged ions flow in opposite directions parallel to the field, generating the electric current density

$$\mathbf{j}=\frac{e}{V}\sum_{i=1}^{N} z_i \mathbf{v}_i , \tag{5}$$

where V is the volume of the system and $\mathbf{v}_i=\mathbf{p}_i/m_i$ is the velocity of the ith ion. Electric conductivity σ is defined as the ratio of the current density to the field

$$\sigma=j_x/E_{\text{EL}} . \tag{6}$$

For weak enough fields (linear response region) it is independent of field strength and equal to the equilibrium value obtained from the Green–Kubo integral[18]

$$\sigma=\frac{V}{3k_BT}\int_0^\infty C_{jj}(t)dt, \tag{7}$$

where C_{jj} is the equilibrium current autocorrelation function

$$C_{jj}(t)=\langle \mathbf{j}(t)\cdot\mathbf{j}(0)\rangle_{EQ} . \tag{8}$$

In equilibrium, when $E_{\text{EL}}=0$, all thermostats give the same statistics in the thermodynamic limit. We have performed the equilibrium simulations with constant kinetic temperature (1) and the Gauss kinetic thermostat. The production runs started from the equilibrated configuration and lasted for 8 ns, with a time window of 5 ps, within which the integral (7) reached a plateau value. The time step was 1 fs. The conductivity was found to be $\sigma=4.53\pm0.05$ mho/cm. The current correlation function (8) is shown in Fig. 2(a). It has a negative minimum corresponding to backscattering and a negative long-time tail.

In an alternating electric field of sufficiently small amplitude in the x direction, time-dependent current density is given by the linear response formula[19]

$$\langle j_x(t)\rangle=\frac{V}{k_BT}\int_0^t ds\, C_{jj}(s)E_{\text{EL}}(t-s), \tag{9}$$

or in the Fourier transformed form

$$\langle \tilde{j}_x(\omega)\rangle=\tilde{\sigma}_0(\omega)\tilde{E}_{\text{EL}}(\omega), \tag{10}$$

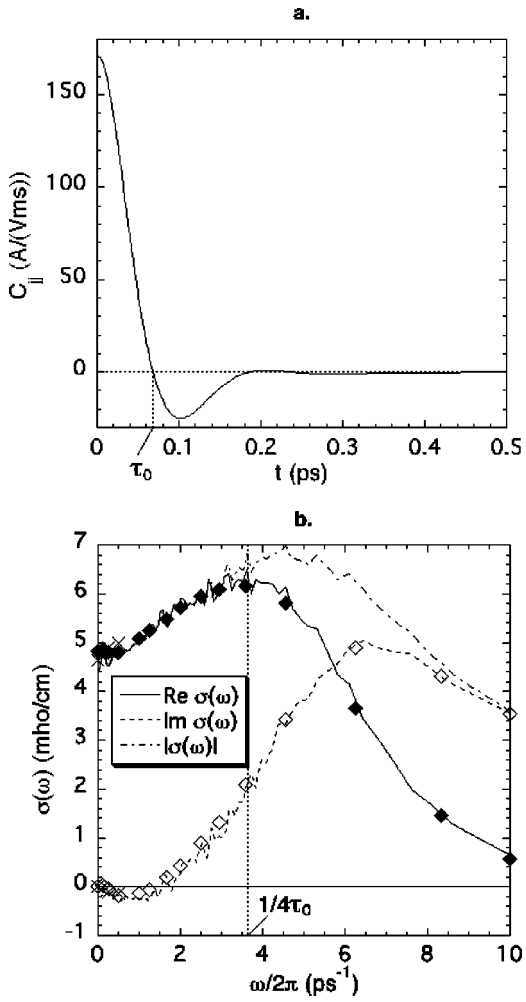

FIG. 2. (a) Equilibrium current autocorrelation function $C_{jj}(t)$. (b) Spectral density of the current autocorrelation function (full and dotted lines) and results of nonequilibrium simulations obtained with kinetic thermostat (diamonds) and configurational thermostat (crosses), in the linear response limit with electric field of the amplitude 1.22×10^9 V/m.

where $\langle \tilde{j}_x(\omega)\rangle$ and $\tilde{E}_{\text{EL}}(\omega)$ are the Fourier–Laplace transforms of the ensemble-averaged current and field, respectively

$$\langle \tilde{j}_x(\omega)\rangle=\int_0^\infty dt\, e^{-i\omega t}\langle j_x(t)\rangle, \tag{11a}$$

$$\tilde{E}_{\text{EL}}(\omega)=\int_0^\infty dt\, e^{-i\omega t}E_{\text{EL}}(t), \tag{11b}$$

and $\tilde{\sigma}_0(\omega)$ is the complex spectral density of the current autocorrelation function

$$\tilde{\sigma}_0(\omega)=\int_0^\infty dt\, e^{i\omega t}C_{jj}(t). \tag{11c}$$

The lower limit of the integrals (11) is zero because of causality. The field $E_{\text{EL}}(t)$ is assumed to be switched on at $t=0$, and the response $\langle j_x(t)\rangle$ must vanish at earlier times.

The time-dependent response to a weak "monochromatic" electric field $E_{\text{EL}}=E_0\cos\omega_0 t$ of amplitude E_0 and

frequency ω_0 in a "final periodic state," when the transients associated with the switching-on step function have decayed, has the form

$$\langle j_x(t)\rangle = \mathrm{Re}[\tilde{\sigma}_0(\omega_0)]E_0 \cos\omega_0 t - \mathrm{Im}[\tilde{\sigma}_0(\omega_0)]E_0 \sin\omega_0 t.$$

The part of response in phase with the field is determined by the real part of the spectral density, and the out-of-phase part is given by its imaginary part. The amplitude of the response current is $E_0|\tilde{\sigma}(\omega_0)|$, and real and imaginary parts determine the phase relationship between current and field. The phase lag ϕ of the current behind the field is

$$\tan\phi = -\mathrm{Im}[\tilde{\sigma}_0(\omega)]/\mathrm{Re}[\tilde{\sigma}_0(\omega)]. \tag{12}$$

The equilibrium spectral density $\tilde{\sigma}_0(\omega)$ is shown in Fig. 2(b). As observed in previous studies,[3–5] the real part has a well-defined maximum at a frequency $\omega_{\max}\approx 2\pi/4\tau_0$, where τ_0 is the zero of the current correlation function $C_{jj}(t)$ [Fig. 2(a)]. The negative values of the imaginary part obtained for very low frequencies are a consequence of the negative long-time tail of $C_{jj}(t)$. The amplitude $|\tilde{\sigma}(\omega)|$ shows a resonance peak for $\omega_P/2\pi \approx 5\ \mathrm{ps}^{-1}$, which is approximately the characteristic frequency obtained from the Taylor expansion of the positive–negative ion pair potential energy around the bottom of the potential well. This is the frequency ω_P of the "plasmon mode" present as modulation of the tail of the current autocorrelation function.

For $\omega\to\infty$ the response vanishes because the system cannot respond fast enough to the changes of the field. The real part decreases much faster than the imaginary part, so that for $\omega \gg \omega_P$ the response is dominated by the imaginary part. For frequencies much higher than the characteristic frequency ω_P, the current lags by nearly $\pi/2$ after the field. For frequencies $\omega \ll \omega_P$ the response is nearly entirely real, and the current is nearly in phase with the field. This behavior is observed with all thermostats for fields of sufficiently low amplitude E_0, i.e., such that the response to the constant field E_0 is linear [Fig. 2(b)].

In a thermostatted system in a monochromatic electric field $E_{\mathrm{EL}}(t)=E_0\cos\omega_0 t$ in a final periodic state, the rate of heat dissipation can be determined from the rate of change of the equilibrium Hamiltonian H_0 according to the thermostatted equations of motion with the field[7] (2) or (4). With the kinetic-type thermostats

$$\frac{d\langle H_0\rangle}{dt} = V\langle j_x(t)\rangle E_{\mathrm{EL}}(t) - 2\langle K_0(t)\alpha(t)\rangle, \tag{13}$$

where K_0 is the total kinetic energy of the system, $K_0 = \Sigma_i \mathbf{p}_i^2/m_i$, and with the configurational thermostat

$$\frac{d\langle H_0\rangle}{dt} = V\langle j_x(t)\rangle E_{\mathrm{EL}}(t) + \frac{1}{T_0}\left\langle s\sum_{i=1}^{N}\mathbf{F}_i\cdot\frac{\partial T_{CONF}}{\partial \mathbf{r}_i}\right\rangle. \tag{14}$$

Equations (13) and (14) can be identified as the first law of thermodynamics. The left-hand side (lhs) represents the rate of change of internal energy, the first term on the right-hand side (rhs) is the rate at which the field does work on the system, and the second term on the rhs is the rate of heat dissipation. In the final time-periodic state, the instantaneous ensemble average on the lhs need not necessarily vanish, but its time average over one period must be zero. In this case, the average dissipation rate $\overline{\dot{Q}_\tau}$ over one period τ (where the bar denotes the time average) is for all types of thermostats in the linear response limit

$$\overline{\dot{Q}_\tau} = VE_0^2\,\mathrm{Re}[\tilde{\sigma}_0(\omega_0)]/2. \tag{15}$$

The real part of spectral density determines the rate of dissipation in analogy with the inverse resistance in an RLC circuit. It is therefore often called frequency-dependent conductivity. The ratio of the amplitude of the current and the amplitude of the field is equal to the modulus of the spectral density $|\tilde{\sigma}_0(\omega_0)|$.

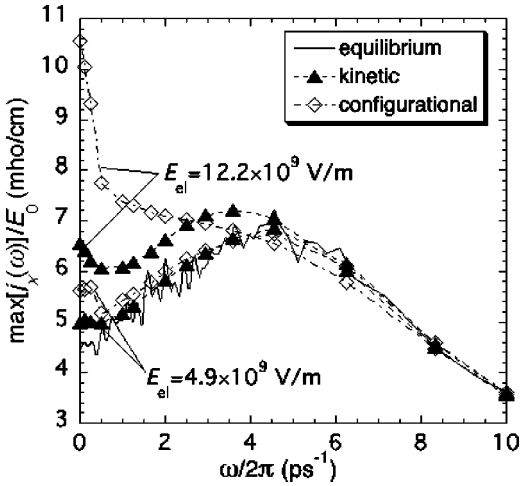

FIG. 3. Frequency dependence of the ratio of the maximum current within the period and the field amplitude for two electric field amplitudes.

V. NONLINEAR RESPONSE IN AN ALTERNATING FIELD

A. Current

In the nonlinear response regime, the ratio of the maximum value of the current within one period, $\max[j_x(\omega_0)]$ and amplitude of the field E_0 is not equal to the absolute value of the equilibrium spectral density at the field frequency ω_0. This occurs because the time-periodic current pattern contains not only the frequency of the monochromatic field but also the higher harmonics, i.e.,

$$j_x(t) = \sum_{n=1}^{\infty} a_n \cos n\omega_0 t + \sum_{n=1}^{\infty} b_n \sin n\omega_0 t, \tag{16}$$

such that a_n and b_n are not negligible for $n>1$, and also because the weights of first harmonic a_1 and b_1 are not equal to $E_0\,\mathrm{Re}[\tilde{\sigma}_0(\omega_0)]$ and $E_0\,\mathrm{Im}[\tilde{\sigma}_0(\omega_0)]$, respectively. Higher harmonics have no influence on dissipation; the heating rate over one period is proportional to the ratio of the real part of the first harmonic a_1 and the field amplitude E_0, which we shall call nonlinear conductivity.

In Fig. 3 we compare the maximum value of the current over one period divided by the field amplitude,

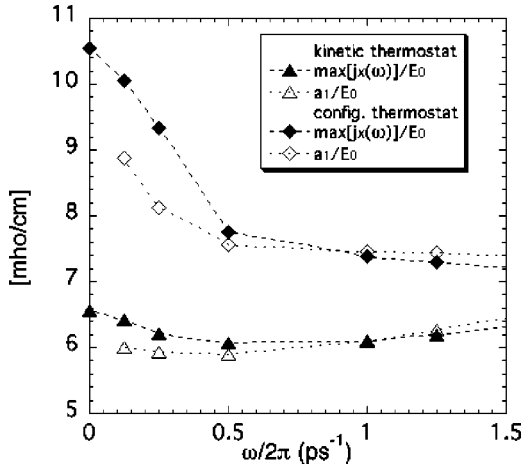

FIG. 4. For the field amplitude 12.2×10^9 V/m in the low-frequency part of the spectrum, the ratio of maximum current and the field amplitude converges to the constant-field (dc) conductivity, while the ratio of the real part of the first harmonic and the field amplitude does not converge to the same limit.

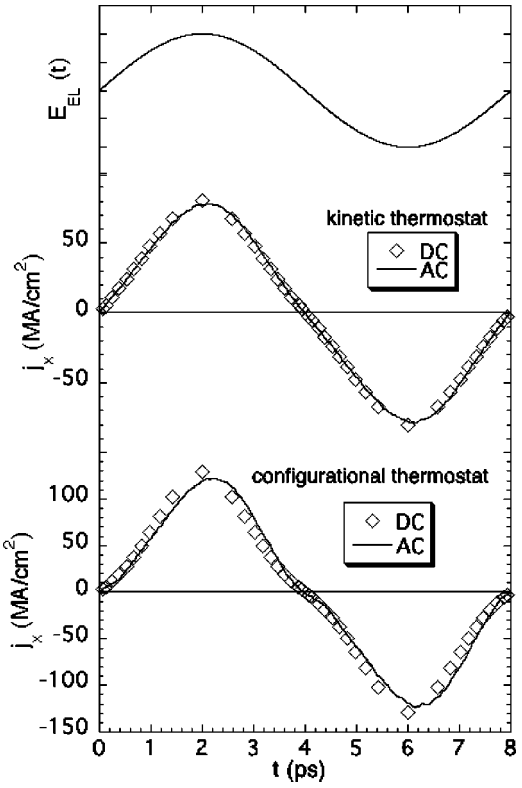

FIG. 5. Top: electric field of sinusoidal form (arbitrary units); middle (kinetic thermostat), and bottom (configurational thermostat): full line—the current form in the alternating field; diamonds—current specified by the dc electric conductivity corresponding to the instantaneous magnitude of the field. In both cases the field amplitude is 12.2×10^9 V/m, and the period of the field is 8 ps.

$\max[j_x(\omega_0)]/E_0$, to the equilibrium spectral density for electric fields of two amplitudes of 4.8×10^9 V/m and 12.2×10^9 V/m for a range of frequencies. For high frequencies $\omega/2\pi\geqslant10$ ps^{-1} the response is linear for both field amplitudes. For $E_0=4.8\times10^9$ V/m with kinetic thermostat it is linear for frequencies $\omega/2\pi\leqslant1.25$ ps^{-1}, while with configurational thermostat small nonlinearities already appear for $\omega/2\pi\leqslant5$ ps^{-1}. As frequency decreases below this value, the amplitude decreases, reaches a minimum, and then increases towards the steady-state value of conductivity for this field. For $E_0=12.2\times10^9$ V/m the differences between responses with two thermostats at low frequencies are much more prominent and start to show already for $\omega/2\pi\leqslant10$ ps^{-1}. With the kinetic thermostat, as well as for the other kinetic-type thermostats, there is a shift towards lower resonance frequency associated with increased damping, and a more pronounced minimum of amplitude between resonance and zero frequency. With configurational thermostat, resonance disappears altogether and the frequency dependence of the amplitude has an overdamped appearance, increasing monotonically with the decrease of frequency. The increased attenuation of the current oscillations is the result of longer response time of the system in stronger constant field. Outside the linear response limit, the steady-state current takes longer to develop in stronger electric fields. In addition, response time is much longer and grows faster with field with configurational thermostat than with kinetic thermostat.[2] For frequencies higher than the inverse response time, current cannot attain its steady-state magnitude before the field is reversed, and therefore its amplitude diminishes and the phase lag between current and field increases. As the response time gets longer, this attenuation starts to occur at lower frequencies.

Nonlinear effects become important only at low frequencies. As frequency diminishes, the nonlinear increase in the amplitude of the first harmonic is followed by the appearance of higher harmonics and the distortion of the current pattern. For slowly varying strong fields of amplitude E_0 and frequency $\omega\ll2\pi/\tau_R$, where τ_R is the response time, the ratio of the maximum value of current during a period and the field amplitude, $\max(j_x)/E_0$, converges to the dc conductivity of the system in the constant field of the magnitude E_0, while the ratio of the real part of the first harmonic and the field amplitude a_1/E_0 (nonlinear conductivity) does not converge to the same limit (Fig. 4). This is true for nonlinear behavior with all thermostats, but the difference is more prominent for configurational thermostat, and less important for kinetic thermostat.

At low field frequencies current very nearly attains the instantaneous magnitude predicted by the dc conductivity for the instantaneous field strength (Fig. 5). The current form is closer to harmonic for the kinetic thermostat, while the distortion is stronger for the configurational thermostat. The appearance of higher harmonics at lower frequencies is the consequence of the field dependence of dc conductivity (Fig. 1). Since the dependence of current on field is more nonlinear with configurational thermostat, this $\omega\rightarrow0$ current pattern is more distorted. There is also a weak attenuation and a small phase lag of the current, because the frequency is not sufficiently higher than the inverse response time. If dc conductivity were a constant for the whole range of the constant field strengths up to its amplitude, there would be no distortion of the sinusoidal current form at low frequencies.

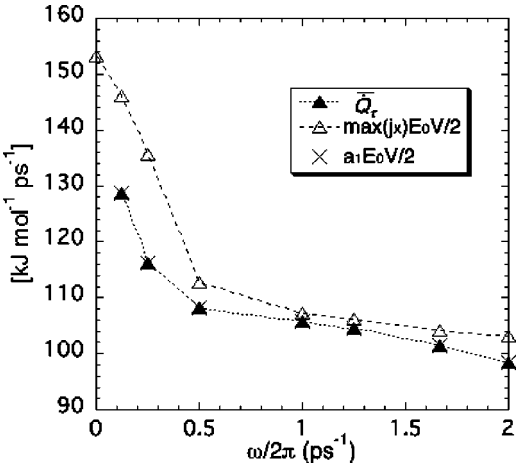

FIG. 6. Average dissipation rate per period from direct calculation (full triangles) and determined by the first harmonic of the current Fourier decomposition (crosses) agree with each other. If current had the harmonic form of the amplitude equal to max$[j_x(t)]$ (empty triangles), the dissipation would converge to half the dissipation rate in the constant field (shown here as $\omega=0$). Data points are in the field of amplitude 12.2×10^9 V/m with the configurational thermostat.

B. Dissipation

In the steady state in a constant field E_0, the dissipation rate $\bar{\dot{Q}}$ is equal to

$$\bar{\dot{Q}}=V\langle j_x\rangle E_0, \tag{17}$$

where $\langle j_x\rangle$ is the steady-state current, twice the value of the average dissipation over one period in the linear response regime (15). In the nonlinear response regime, where current density has the form (16), the average dissipation over one period of the field is determined by the real part of the first harmonic

$$\bar{\dot{Q}}_\tau=VE_0a_1/2. \tag{18}$$

In the zero-frequency limit $\omega\to0$, a_1 is the real part of the first harmonic in the Fourier expansion of the current form generated using field-dependent dc conductivity (as in Fig. 5). Therefore, the average dissipation rate over one period for nonlinear response in alternating field does not converge to half the dc dissipation rate in the field E_0 (Fig. 6) in the low-frequency limit. On the other hand, the maximum value of the current in the low-frequency limit max$[j_x(\omega_0)]$ is equal to the steady-state current $\langle j_x\rangle$ in (17), and thus the maximum instantaneous rate of work done by the field converges to the steady-state dissipation (17).

The rate at which the field does the work and the dissipation rate generally do not match instantaneously. We compare the time-dependent patterns of the rate of change of the unperturbed Hamiltonian $\dot{H}_0(t)$, the dissipation rate $\dot{Q},(t)$ and the work rate $\langle j_x(t)\rangle E_{EL}(t)V$ for a high, intermediate, and low frequency in the field of the higher amplitude $E_0=12.2\times10^9$ V/m in Fig. 7. The dissipation rate $\dot{Q}$ is negative for all frequencies at all times, which means that heat is being removed throughout the field cycle, regardless of the sign of the work rate. For very high frequencies ($\omega/2\pi=10$ ps^{-1}) the modulation of dissipation is the smallest, and the phase behavior is such that the least heat is extracted when the work rate is the highest. At intermediate frequencies the phase lag between work rate and dissipation shifts so that the modulation of the rate of change of the Hamiltonian decreases, until at low frequencies ($\omega/2\pi\leqslant0.125$ ps^{-1}) the rate of dissipation is nearly opposite the work rate. The internal energy H_0 is, however, not constant even in the $\omega\to0$ limit, because the instantaneous value of total energy has to correspond to its value in the constant electric field of instantaneous magnitude. The energy would be constant, and $\dot{H}_0=0$, only in the linear response limit, when work and dissipation would become exactly opposite in the zero frequency limit.

When heat is removed to the environment at a constant temperature T, entropy of the environment increases at the rate $\dot{S}=-\dot{Q}/T$. Since $\dot{Q}(t)$ is always negative, heat is always transmitted to environment and not vice versa.

There is an important technical point regarding the use of Nosé–Hoover-type thermostats for temperature control far from equilibrium. In a constant field in a steady state, the value of the constant σ^2/τ_{TC}^2 affects the time scale of fluctuations, but not their magnitude or statistical distribution. In principle, for large systems, one obtains the same averages over infinite sampling time regardless of the value of the constant. For finite sampling times, the averaging time has to be longer when the constant is smaller. The main criterion for the choice of the value of σ^2/τ_{TC}^2 is that it should be large enough to allow good statistics for averaging times that are not forbiddingly long, while at the same time not affecting numerical stability of the equations (4).

In explicitly time-dependent external fields, the constant σ^2/τ_{TC}^2 has to be chosen more carefully. In this case there are two additional inherent time constants, the period of the field and the response time of the system. They determine the rate of work done by the field and therefore the rate of dissipation needed in order to keep the temperature constant. This becomes especially important for the fields of large amplitude and high frequency where at some points in the field cycle the work rate becomes very large. If the Nosé–Hoover time τ_{TC} is too long, the numerical feedback cannot extract enough heat at this time and makes up for it at later times when the work rate is smaller. In this case temperature is not constant during the field cycle, but has a periodic time dependence around the desired mean value T_0 [Fig. 8(a)]. This causes the values of $\langle j_x(t)\rangle$ and $H_0(t)$ to overshoot the values prescribed by the steady-state response at T_0 and changes the phase lag between current and field. As a consequence, dissipation can become positive at some subintervals of the field, meaning that heat is being put into the system from the environment and that entropy increases [Fig. 8(b)]. In Fig. 8 the Nosé–Hoover constant σ^2/τ_{TC}^2 was chosen as 100 Å^2/ps^2 as in lower response (lower field, higher frequency) simulations, and the time step was 0.5 fs. In Fig. 7(b), the Nosé–Hoover constant was 1000 Å^2/ps^2. The time step in this case needed to be reduced to 0.1 fs.

One is tempted to attach some physical meaning to parameters in the thermostat term, e.g., to the response time τ_{TC}. It is important to keep in mind that the thermostat is introduced as a numerical device that should only account

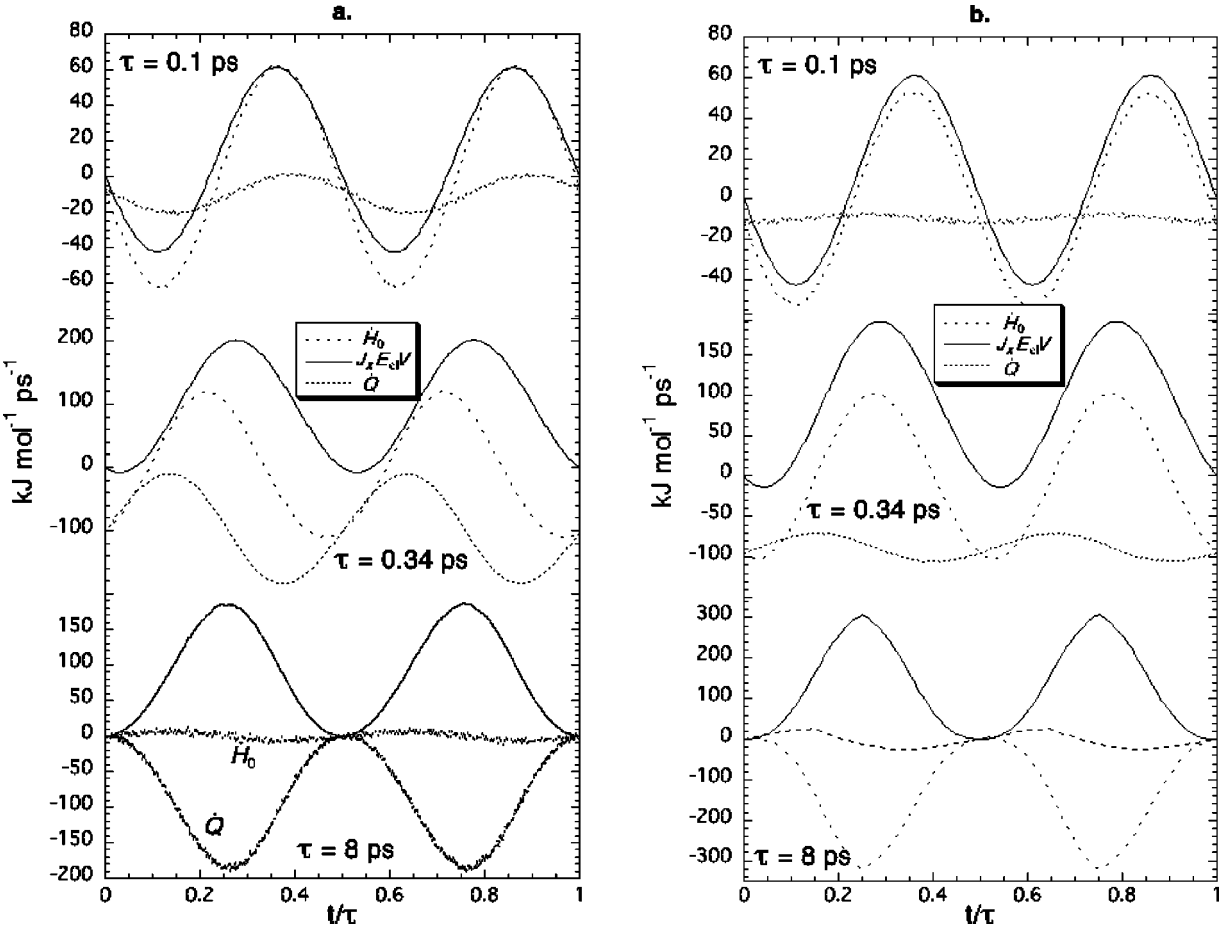

FIG. 7. Instantaneous relationship between dissipation, work rate, and the rate of change of equilibrium Hamiltonian during one period for kinetic (a) and configurational (b) thermostat for high (top), intermediate (middle), and low (bottom) frequencies.

for the final effects of dissipation (i.e., keeping a chosen microscopic expression for temperature constant) and not to reproduce any aspect of its real mechanisms. The response time should be chosen so that the temperature conservation is valid at all times. If the thermostat fails to do so, as in Fig. 8 where temperature oscillates periodically around the mean value with large amplitude, the results will be incorrect.

VI. CONCLUSION

We have investigated the conductivity of molten sodium chloride in alternating electric fields of large amplitude for a large range of frequencies, using two types of thermostat, and compared it to the spectral density of the equilibrium current autocorrelation function. The current correlation function has a negative long-time tail, which makes the imaginary part of the spectral density negative in a low-frequency range. This result has been verified by NEMD simulation in an electric field of small amplitude $E_0 = 1.22 \times 10^9$ V/m, for which the response is linear with both thermostats in the whole investigated range of frequencies.

For any given field amplitude, the response is always linear for sufficiently high frequencies. Nonlinearities appear at lower frequencies for smaller field amplitudes, and are manifested in the nonlinear increase in the amplitude of the first harmonic of the Fourier expansion of the periodic current form and the distortion due to the appearance of higher

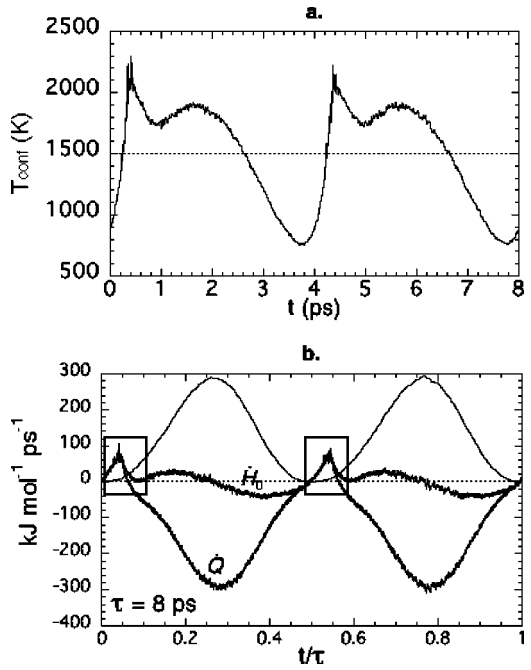

FIG. 8. (a) Periodic dependence of the configurational temperature and (b) dissipation, work rate, and the rate of change of equilibrium Hamiltonian during one period in the field of amplitude 12.2×10^9 V/m and frequency $\omega/2\pi = 0.125$ ps^{-1}, when the feedback constant is too small ($\sigma^2/\tau_{TC}^2 = 100$ Å^2/ps^2). In the time intervals within the rectangles the entropy decreases.

harmonics. Response is more nonlinear with the configurational thermostat than with the kinetic thermostat. All these effects can be understood from the different nonlinear field dependence of current and the rate of increase of the response time with field in a constant electric field for the two thermostats.[2]

In the linear response limit, dissipation rate is determined by the real part of the equilibrium spectral density of the current correlation function at the field frequency. For $\omega \rightarrow 0$ the average dissipation per period approaches half the steady-state dissipation in a constant field of the magnitude equal to the alternating field amplitude. When the response is not linear, average dissipation per period does not converge to this limit. It is determined by the first harmonic in the Fourier decomposition of the anharmonic periodic current pattern obtained from nonlinear conductivity at the instantaneous value of the field.

The average dissipation rate is similar for the two thermostats except for the lowest frequencies. At high frequencies, the rate of change of internal energy is nearly in phase with the work rate, and dissipation is nearly constant over the period. At low frequencies the work rate and the dissipation rate are nearly opposite, but generally of a different shape. The difference is equal to the periodic change of the equilibrium Hamiltonian, obtained from its dependence on the instantaneous value of the field. In the linear response regime in the zero-frequency limit, the work and dissipation rate would be exactly opposite and internal energy would be constant.

ACKNOWLEDGMENT

The authors wish to thank the Australian Partnership for Advanced Computing for a substantial allocation of computer time for this project.

[1] J. Delhommelle and J. Petravic, J. Chem. Phys. **118**, 2783 (2003).
[2] J. Petravic and J. Delhommelle, J. Chem. Phys. **118**, 7477 (2003).
[3] J.-P. Hansen and I. R. McDonald, Phys. Rev. A **11**, 2111 (1975).
[4] J. Trullàs and J. A. Padró, Phys. Rev. B **55**, 12210 (1997).
[5] I. M. Svishchev and P. G. Kusalik, Phys. Chem. Liq. **26**, 237 (1994).
[6] S. R. de Groot and P. Mazur, *Non-equilibrium Thermodynamics* (Dover, New York, 1984).
[7] D. J. Evans and G. P. Morriss, *Statistical Mechanics of Non-Equilibrium Liquids* (Academic, London, 1990).
[8] W. G. Hoover, *Computational Statistical Mechanics* (Elsevier, New York, 1991).
[9] D. MacGowan and D. J. Evans, Phys. Rev. A **34**, 2133 (1986).
[10] J. Delhommelle, J. Petravic, and D. J. Evans, Phys. Rev. E **68**, 031201 (2003).
[11] H. H. Rugh, Phys. Rev. Lett. **78**, 772 (1997); J. Phys. A **31**, 7761 (1998).
[12] J. Delhommelle and D. J. Evans, J. Chem. Phys. **115**, 43 (2001).
[13] L. Lue, O. G. Jepps, J. Delhommelle, and D. J. Evans, Mol. Phys. **100**, 2387 (2002).
[14] M. P. Tosi and F. G. Fumi, J. Phys. Chem. Solids **25**, 31 (1964).
[15] Y. Guissani and B. Guillot, J. Chem. Phys. **101**, 490 (1994).
[16] S. W. de Leeuw, J. W. Perram, and E. R. Smith, Proc. R. Soc. London, Ser. A **373**, 27 (1980).
[17] M. P. Allen and D. J. Tildesley, *Computer Simulation of Liquids* (Clarendon, Oxford, 1987).
[18] J. P. Hansen and I. R. McDonald, *Theory of Simple Liquids* (Academic, London, 1986).
[19] R. Zwanzig, *Non-equilibrium Statistical Mechanics* (Oxford University Press, Oxford, 2001).